ISSN 1027-5495. Functional Materials, 30, No.1 (2023), p. 104-114.
doi:https://doi.org/10.15407/fm30.01.104

Effect and mechanism of action of glass waste powder as an additional binder on the properties of recycled concrete

Qidong Wang[1], Minghua Yang[2], Xudong Wang[1]

[1]Yuanpei College, Shaoxing University, 312000 Shaoxing, China
[2]Shaoxing Yuelu Traffic Engineering Co., Ltd, 312000 Shaoxing, China

Received December 28, 2022

As an additional binder, glass powder (GP) is a good replacement for cement in the production of recycled aggregate concrete (RAC), which is beneficial for recycling solid waste resources and reducing environmental pollution. The effects of 10 %, 20 % and 30 % by weight of GP which partially replaces cement on the compressive strength, splitting strength, elastic modulus, drying shrinkage, and creep of RAC were studied; the internal microstructure was also analyzed by MIP and nanoindentation techniques. The results show that GP reduces the compressive strength, splitting strength and elastic modulus of RAC at the early stage, while at the later stage, the compressive strength and elastic modulus for RAC containing 10 % and 20 % GP are higher than those of the control group. In addition, a GP additive reduces the drying shrinkage and creep of RAC, and the sample containing 10 % GP shows the best effect. Due to the pozzolanic effect and the effect of microaggregate filling of GP, the microstructure of the RAC matrix and the interfacial transition zone (ITZ) improves.
Keywords: glass powder, recycled aggregate concrete, drying shrinkage, creep, microstructure.

Вплив та механізм дії порошку скляних відходів як додаткового віяжучого на властивості оборотного бетону. *Qidong Wang, Minghua Yang, Xudong Wang*
Як додатковий сполучний, склопорошок (GP) є хорошою заміною цементу у виробництві вторинного заповнювача бетону (RAC), який є корисним для переробки ресурсів твердих відходів та зменшення забруднення навколишнього середовища. Досліджено вплив 10 %, 20 % і 30 % маси ГП, який частково замінює цемент, на міцність при стиску, міцність на розщеплення, модуль пружності, усадку при висиханні та повзучість RAC; внутрішня мікроструктура також була проаналізована методами MIP та наноіндентування. Результати показують, що GP знижує міцність на стиск, міцність на розщеплення та модуль пружності RAC на ранній стадії, тоді як на пізній стаді міцність на стиск і модуль пружності для RAC, що містить 10 % і 20 % GP, вищі, ніж у контрольної групи. Крім того, добавка GP зменшує усадку при висиханні та повзучість RAC, а зразок, що містить 10 % GP, демонструє найкращий ефект. Завдяки пуцолановому ефекту та ефекту мікроагрегатного заповнення ГП покращується мікроструктура матриці РАК та міжфазної перехідно зони (МПЗ).

1. Introduction

Recycled aggregate concrete (RAC) is a sort of green concrete [1]. Studies show that the flexural strength [2], shear strength [3] and fatigue resistance of RAC decreases to different degrees with increasing the replacement rate of recycled aggregate [4]. In general, the RAC shows lower mechanical properties than natural aggregate [5–7]. The RAC compressive strength is reduced by 20 % ~ 40 %, when reclaimed material completely replaces natural aggregate [8, 9]. Silva et al. [10] found that the elastic

Table 1. Chemical properties of cement and GP

Sample	Chemical composition (%)						
	K_2O	SO_3	MgO	CaO	SiO_2	Al_2O_3	Fe_2O_3
Cement	0.35	2.30	2.08	60.24	21.82	4.54	3.20
GP	0.82	0.05	2.37	5.51	88.52	2.24	0.046

modulus of RAC containing 20 % and 100 % recycled aggregate decreased by 20 % and 40 %, respectively. Mechanical properties are the most fundamental properties of RAC, and the volumetric stability of RAC is as essential as its mechanical properties. In structural analysis and design, the volume stability of concrete must be taken into account to ensure the safety and maintainability of buildings. Unfortunately, the mechanical properties and volumetric stability of RAC are not satisfactory, and the addition of supplementary cementing materials (SCMs) is a traditional solution to improve the RAC properties. Previous reports have confirmed that SCMs significantly affect the mechanical performances and volume stability of RAC and show good ecological and economic effects [11, 12].

Currently, waste glass (WG) accounts for 7 % of the total solid waste in our country. In theory, glass products can be completely recycled, but the differences in composition and physical properties of different glass products make the recycling very difficult and uneconomical, and only a small part is recycled. At present, the main disposal method of glass waste is still landfill, but since glass is a non-biodegradable material, its landfill method will cause serious pollution to the environment. The treatment of WG has become an urgent environmental problem. In recent years, scientists have explored WG preparation as an aggregate for an application in concrete. Since WG is prone to alkali-aggregate reactions in an alkaline environment, the performance of concrete is reduced, which leads to the unsatisfactory effect of WG using as a coarse and fine aggregate in concrete [13, 14]. Fortunately, studies show that the WG ground powder (GP) instead of cement can improve mechanical properties [15], durability [16] and micro-structure of concrete [17, 18]. It is reported that the pozzolanic effect of GP and the high strength and elastic modulus of GP improve mechanical properties of concrete and potentially replace silica fume [19]. Schwarz et al. [20] pointed that the replacement of cement with 10% GP showed the best mechanical properties, and GP also had the ability to enhance durability of concrete. Omran et al. [21] pointed out that after replacing part of the cement with GP, the strength of concrete decreased in the early stage; but after 91 days, the strength of concrete was significantly improved, and the frost resistance was also enhanced. Wang et al. [22] found that adding GP improved the slurry microstructure compaction and reduced the porosity. Aliabdo et al. [23] found that GP has a pozzolanic effect, which does not significantly affect the expansion of the cement and reduces the drying shrinkage of the mortar [24]. Islam et al. [25] believe the use of GP instead of 20 % cement is compelling in terms of economic and environmental issues. The above studies confirm that GP applied as SCMs exhibits a satisfactory pozzolanic effect.

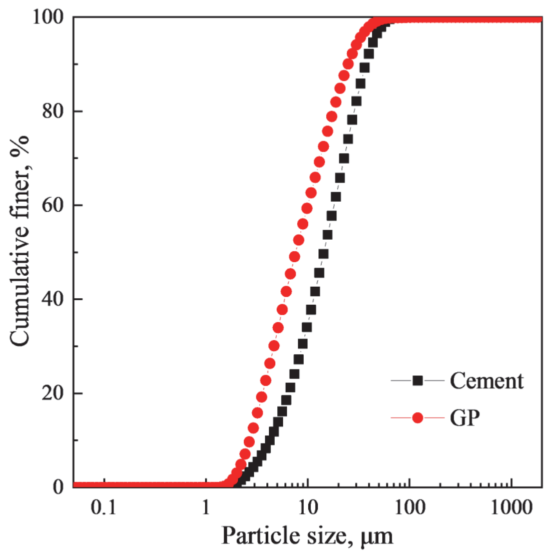

Fig. 1. Particle size distribution of cement and GP.

With too much WG produced worldwide, the demand for GP as an SCM to replace cement is on the rise. However, the current research on GP mainly focuses on the performance of ordinary concrete, and there is no relevant report on the performance of RAC, especially the volumetric stability. Therefore, the influence of GP on the compressive strength and elastic modulus of

Table 2. Design mix ratio of RAC (kg/m^3)

Sample	Cement	GP	Water	Sand	NCA	RCA	PS
R-0GP	450	0	160	714	534	534	4.06
R-10GP	405	45	160	714	534	534	4.35
R-20GP	360	90	160	714	534	534	4.62
R-30GP	315	135	160	714	534	534	4.62

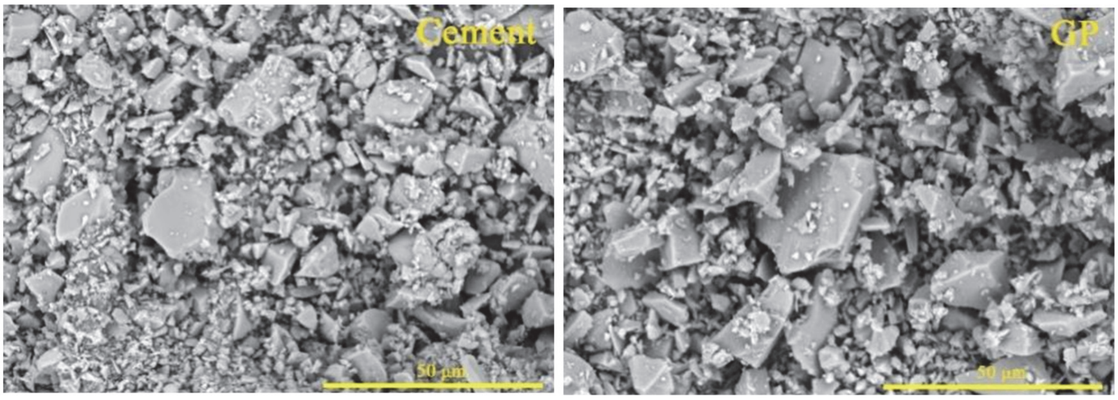

Fig. 2. SEM images of cement and GP.

RAC is studied in this paper. Then, drying shrinkage and creep of recycled concrete containing GP were studied. Finally, the evolution of RAC microstructure was investigated by the mercury injection method (MIP) and the nanoindentation technique to reveal the mechanism of GP action on the RAC volume stability.

2 Raw material and tests

2.1 Raw material

In this study, P·O 42.5 cement was used, which complies with the Chinese standard GB175-207. GP is obtained by milling WG. Table 1 shows the chemical components of cement and GP. The table shows that GP contains a large amount of SiO_2 and a small amount of CaO. Fig. 1 shows that the particle size of GP is significantly smaller than that of cement particles. It can be observed from Fig. 2 that the micromorphology of GP and cement is irregular-block. The specific gravities of cement and GP are 3050 kg/m^3 and 2490 kg/m^3, respectively. The recycled aggregate after concrete crushing is taken as a coarse aggregate with particle size range of 5 ~ 20 mm, and the specific gravity of 2450 kg/m^3. River sand is a fine aggregate with specific gravity of 2530 kg/m^3. Polycarboxylate superplasticizer (PS) was applied as an additive, and the water-reducing rate is 25 %. Tap water is stirred water.

2.2 Mix ratio design and preparation

To study the effect of GP on the volume stability of RAC, four various GP contents of 0 %, 10 %, 20 % and 30 % were designed. The w/b ratio of RAC is 0.4. In addition, the slump of RAC was maintained at 160 ~ 200 mm by adjusting the dosage of PC. The mix ratio of RAC is shown in Table 2.

2.3 Test method

The compressive strength was measured on a RAC cube with a side of 150 mm. A specimen of 100 mm × 100 mm × 300 mm was used to test the modulus of elasticity, shrinkage on drying and creep.

Firstly, the specimens were molding according to the mixing ratio in Table 2; then they were cured at room temperature for 24 h. After demoulding, the samples were stored in the standard curing chamber for curing of the appropriate age until the mechanical properties were tested. For drying shrinkage and creep measurements, the specimens were placed in a conventional curing chamber for 6 days after demoulding, and immediately placed on a drying machine for shrinkage and creep testing at T = 20±2° and relative humidity RH = 60±5 % indoors. A separate test was carried out on each specimen to eliminate the influence of drying shrinkage on creep strain.

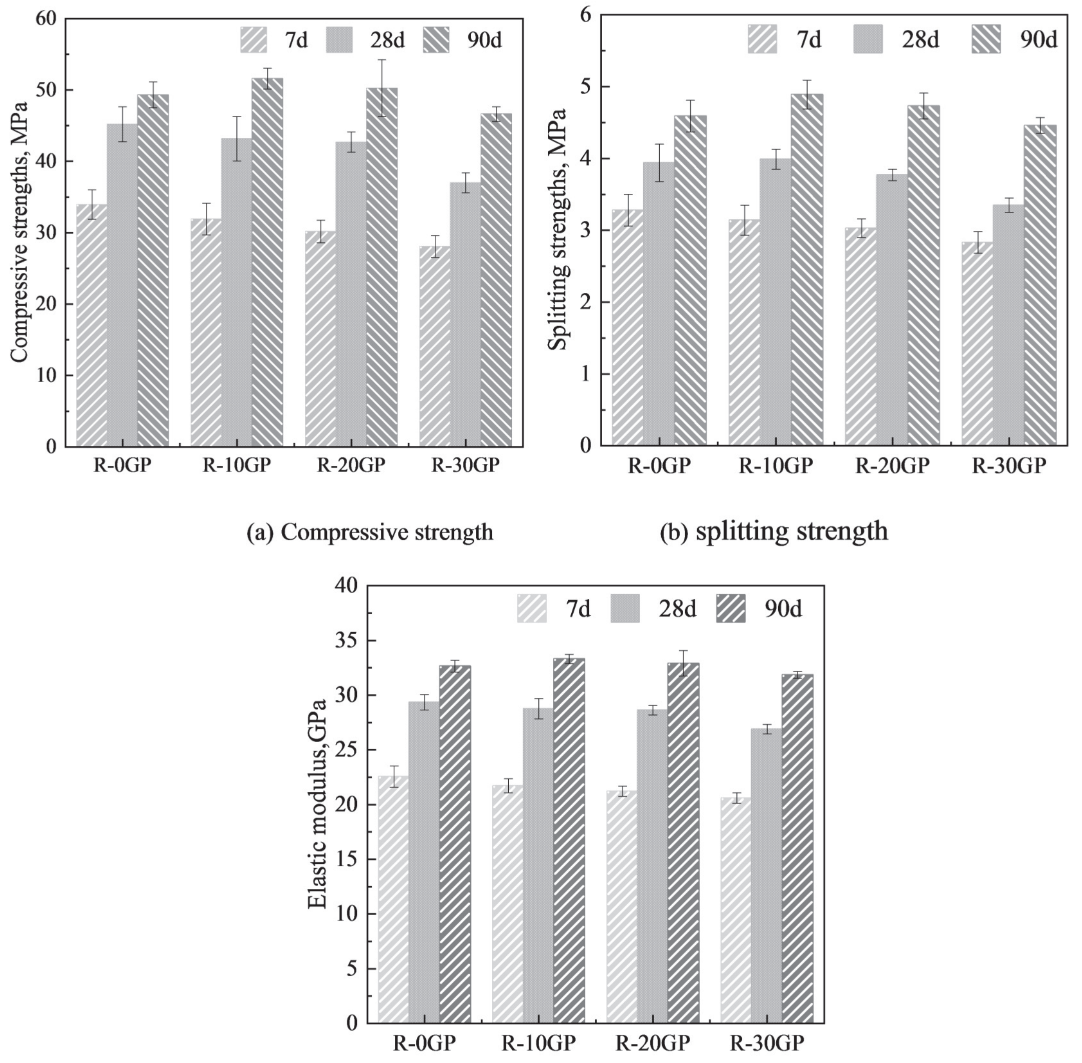

(a) Compressive strength (b) splitting strength

(c) Modulus of elasticity

Fig. 3. Effect of GP on mechanical properties of RAC.

The difference between the creep test results and the dry shrinkage was used to calculate the creep strain value.

Using the mercury intrusion porosimetry (MIP) method, the pore structure of RAC was studied. The test materials were small pieces of 3–5 mm in diameter made of mortar and fine aggregate and submerged in an ethanol solution for 7 days to stop hydration. Prior to MIP testing, specimens were dried and kept in airtight containers. The changes of phase composition of RAC specimens were measured by nano-indentation technique. The detailed process is described in [26].

3. Results

3.1 Mechanical properties Figure 3a shows the effect of different GP contents on the compressive strength of RAC. The RAC compressive strength decreased gradually with increasing GP content in the early stage. With increasing age, the compressive strength of specimens containing GP slowly approached the control group. The compressive strength of the specimen containing 10 % GP cured for 90 days was the highest. It is important to note that GP exhibits little pozzolanic effect and only has an early microfilling effect, resulting in a reduction in RAC compressive strength. In the later stage, the pozzolanic effect of GP is activated and it reacts with CH molecules produced by cement hydration to form more C–S–H gels [28]. Meanwhile, the unreacted GP acts as a microaggregate to fill the pores. Consequently, the pozzolanic effect combined with the micro aggregate filling effect of GP contributes to the increase in the compressive strength of the RAC at a later stage. However, the higher GP content resulted in the formation of only a small amount of CH, which could not effectively contribute to the pozzolanic effect of GP, resulting in a decrease in the compressive strength of the RAC.

As seen in Fig. 3b, the early (7d) splitting strength of the RAC with 10 %, 20 %, and 30 % GP is reduced by 4.2 %, 7.6 %, and 13.7 %, respectively, compared with the R-0GP. However, with increasing age, GP can improve the splitting strength of RAC. The splitting strength of the R-10GP specimen after 90 days is 6.5 % higher than that of the R-0GP. However, the further increase in the GP content will have an adverse effect on the splitting strength of RAC, while the splitting strength of R-30GP specimens at different ages is lower than that of the control group. More notably, with the increase of the GP content, the RAC splitting strength decreases less than the compressive strength. This phenomenon may be caused by the angular shape of GP particles, which enhance the setting force and the bonding effect between the aggregate and the matrix, and to a certain extent slow down the decrease in the splitting strength of concrete.

The modulus of elasticity of RAC has the same tendency to change as the compressive strength. The early elastic modulus of RAC decreases with the addition of GP. After 90 days, the modulus of the samples containing 10 % and 20 % GP surpassed the modulus of elasticity of R-0GP, however, the samples containing 30 % GP still had a lower modulus of elasticity than R-0GP. The strengthening effect of GP in a late stage is mainly due to the high strength and elastic modulus of GP, and the pozzolanic effect of GP at the late stage strengthens the microstructure of RAC. He et al. also confirmed that the addition of GP can improve the elastic modulus of concrete, especially at a later stage [29]. The optimal content of GP in this study was 10 %, which was consistent with other experimental results [20]. However, the optimal amount of GP is associated with differences in GP, water-binder ratio, curing conditions and other conditions.

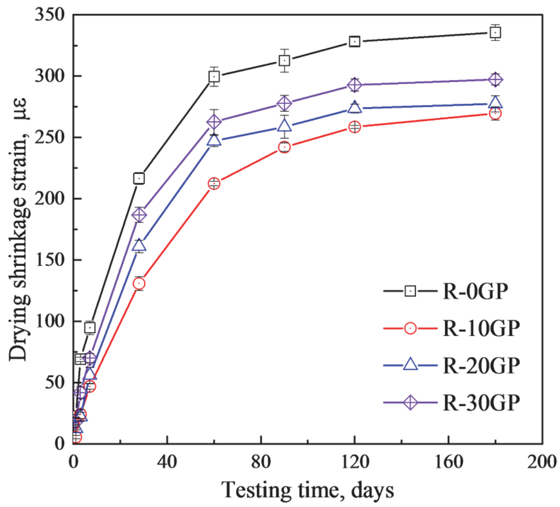

Fig. 4. Effect of GP on RAC drying shrinkage.

The drying shrinkage strain of RAC with various GP contents is shown in Fig. 4. In this figure, all specimens show a similar change trend. At the early stage, the drying shrinkage developed rapidly for all specimens. When the age reaches 60 days, the drying shrinkage of the specimen slows down and tends to be stable gradually. In addition, it is obvious that different GP content has a different effect on the shrinkage of RAC upon drying. In comparison with the R-0GP, after 180 days, the drying shrinkage of specimens with 10 %, 20 % and 30 % GP decreases by 19.7 %, 17.3 % and 11.4 %, respectively.

3.3 Creep

The creep test and the drying shrinkage test were conducted simultaneously. Fig. 5a shows the effect of the different GP content on RAC creep. It can be found that the RAC creep trend is similar to the drying shrinkage trend. Compared to the control group, with cement replacement of 10 %, 20 %, and 30 % GP, the creep of the RAC samples after 180 days was reduced by 26 %, 20 %, and 11.4 %, respectively. Taking into account the effect of vertical stress on creep, a creep factor is introduced to evaluate the effect of GP on the RAC creep. The creep coefficient C_{rc} is the ratio of creep strain ε_{cs} to elastic strain, as shown in Eq. (1):

$$C_{rc} = \frac{\varepsilon_{cs}}{\varepsilon_{es}} = * \frac{\varepsilon_{cs} \cdot E_7}{\sigma} = \frac{4\varepsilon_{cs} \cdot E_7}{f_7}. \quad (1)$$

Here εcs is the creep strain, ε_{es} is the elastic strain, σ is the vertical compressive stress, $0.25f_7$, f_7 is the 7-days compressive strength of the RAC sample, and E_7 is the

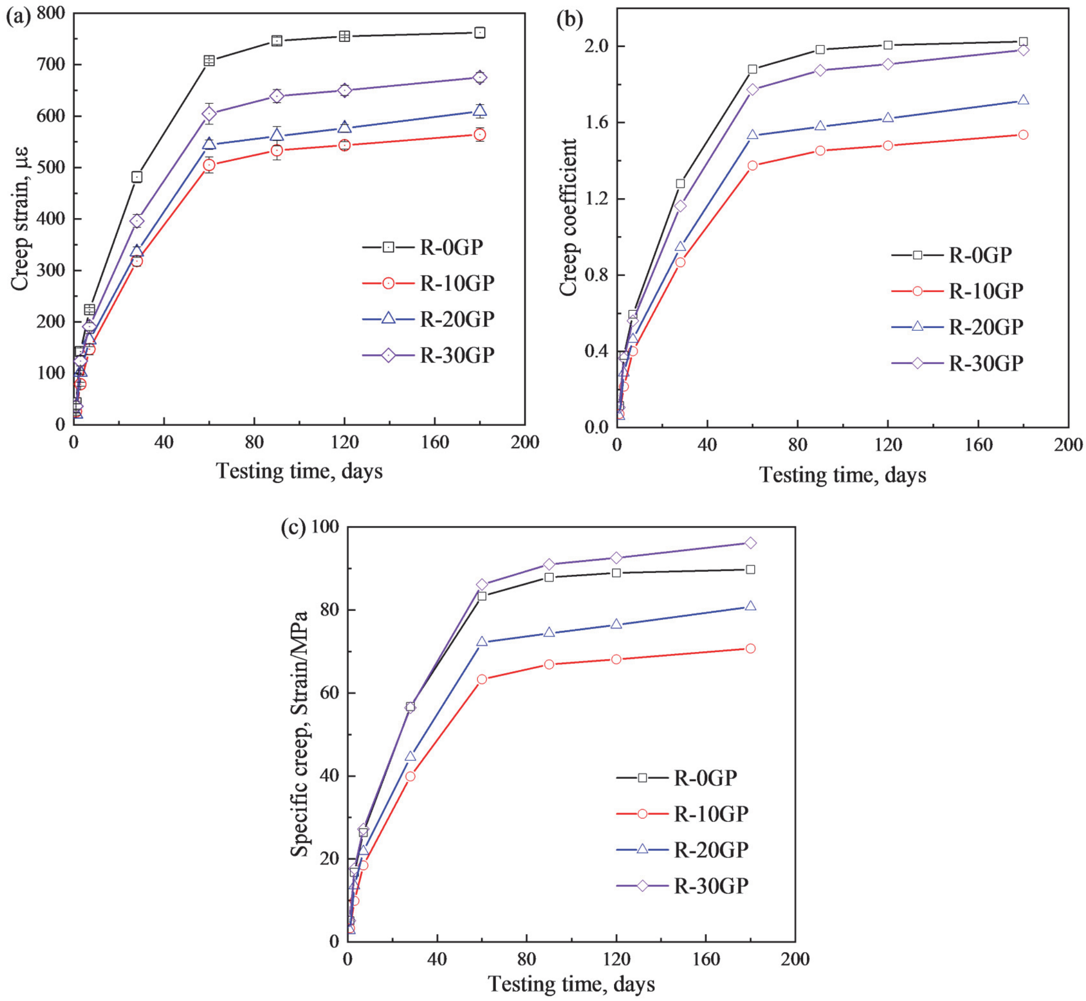

Fig. 5. Effect of GP on RAC creep: (a) creep strain; (b) creep coefficient; (c) creep degree.

7-days elastic modulus of RAC sample. Fig. 5b shows the curves of the creep coefficient versus loading time of specimens containing GP. It can be seen that GP decreases the creep coefficient of RAC. Compared with R-0GP, the creep coefficient for 10 %, 20 % and 30 % GP decreased by 24.4 %, 15.6 % and 2.2 %, Crespectively. Significantly, GP has weakened the effect of improvement of the creep coefficient. This is mainly due to the decrease in the mechanical properties of RAC due to the low pozzolanic effect of GP at an early stage. In addition, a decisive indicator for evaluating the creep property of concrete is the degree of creep, which can be calculated using formula (2). Fig. 5c shows that the incorporation of 10 % and 20 % GP into the RAC can reduce the creep degree. However, adding too much GP increases the degree of RAC creep and the trend towards improvement becomes more significant with age. This is closely related to the lower compressive strength accompanied by elastic modulus of the specimen containing 30 % GP in the early stage.

$$C_{rc} = \frac{\varepsilon_{cs}}{\sigma} = \frac{4\varepsilon_{cs}}{f_7}. \quad (2)$$

3.4 SEM analysis

Fig. 6 shows the effects of different amounts of GP on the microstructure of the interfacial transition zone (ITZ) in RAC. From the figure, it can be seen that some loose C–S–H gels and bulk CH are distributed in the microstructure of the R-0GP specimens, and there are also a few microcracks between the hydration products (Fig. 6a). After adding 10% GP, the C–S–H gels bind forming a dense microstructure, and the number of CH crystals decreases

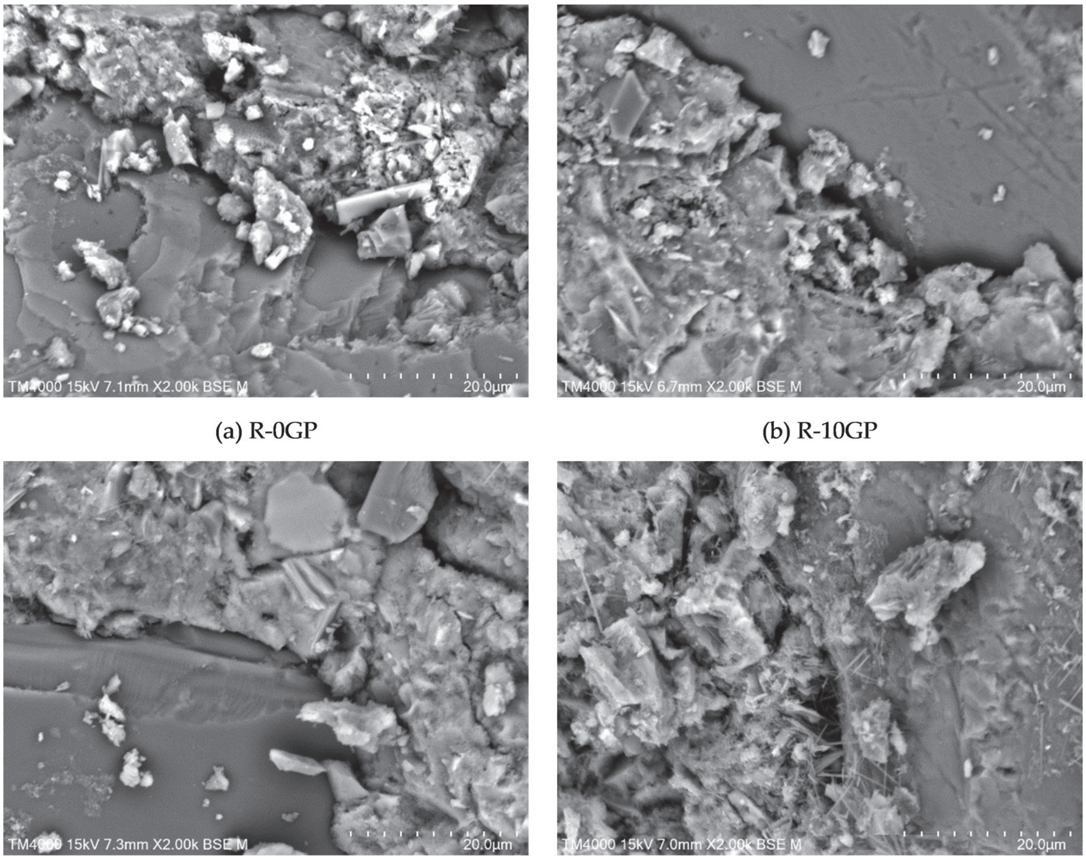

(a) R-0GP (b) R-10GP

(c) R-20GP (d) R-30GP

Fig. 6. SEM-BSE image of RAC at 90d.

(Fig. 6b); this is due to the good pozzolanic effects of GP. More C–S–H gels were formed to fill the pores. However, the effect of GP on improving the microstructure of RAC specimens decreased as the dosage was further increased (Fig. 6c and d), which may be due to the "dilution effect" of cement. The microstructure changes of RAC correspond to the development of mechanical properties mentioned above.

3.5 Pore structure

During the cement slurry hydration process, pores of different sizes are formed. Their size ranges were less than 20 nm, 20 ~ 50 nm, 50–100 nm, and more than 100 nm, respectively [29, 30]. Fig. 7 displays the cumulative porosity curve of specimens, and Table 3 presents the pore size distribution. The results show that the incorporation of GP changes the pore distribution in RAC. With an increase in the GP content in the RAC, the porosity of the specimen increases gradually. When the GP content is 10 %, the specimen shows the lowest total porosity. When the GP content increased to 30 %, the porosity of the specimen was higher than that in the R-0GP specimen. More notably, compared with the R-0GP, the number of pores larger than 100 nm in the specimens containing 10 % and 20 % GP decreased, while specimens containing 30 % GP showed the opposite result; this also explains why specimens containing 10 % GP showed the best me-

Table 3. Pore size distribution in sample containing GP

Samples	<20 nm	20–50 nm	50–100 nm	>100 nm
R-0GP	0.035	0.0484	0.028	0.1185
R-10GP	0.01	0.033	0.042	0.093 R-20GP
R-30GP	0.016	0.0295	0.039	550.152

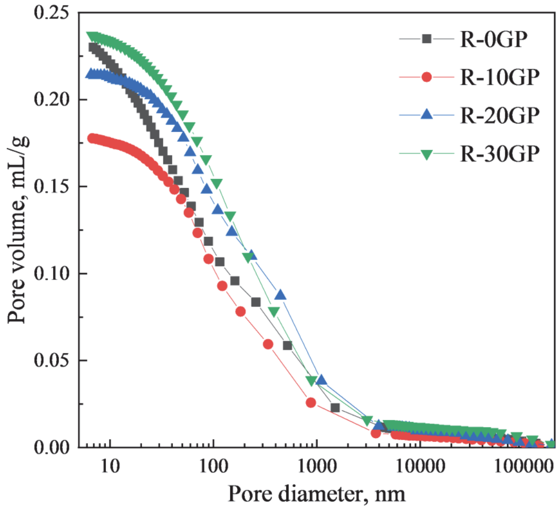

Fig. 7. Effect of GP after 90d on the cumulative porosity of RAC sample.

chanical properties. In addition, incorporating GP reduces the porosity to less than 50 nm, which positively affects the improvement of drying shrinkage and creep.

3.6 Nanoindentation

Fig. 8 shows the distribution of elastic modulus in the ITZ region of RAC specimens. From left to right are new mortar, the ITZ, and old mortar. It can be found that the ITZ is about 45 to 65 μm wide. The elastic modulus of the old mortar is significantly higher than that of the new mortar, and the distribution is uneven, which is attributed to the distribution of some CH in the area of the old mortar. The ITZ width of R-0GP is 65 μm, and the average elastic modulus is 13.5 GPa. However, with the addition of GP, the width of the ITZ in RAC is reduced. ITZ widths are 45 $E mum, 50 μm and 55 μm for R-10GP, R-20GP, and R-30GP specimens, respectively, and ITZ widths of R-10GP, R-20GP, and R-30GP specimens are reduced by 15.4 %, 30.85 and 23.1 respectively, compared with R-0GP specimens. At the same time, due to the good pozzolanic effect of GP, the ITZ microstructure of RAC may be improved, which leads to the improvement of the elastic modulus of ITZ and the new mortar. The ITZ average elastic modulus for R-10GP, R-20GP, and R-30GP specimens are 17.5 GPa, 15.2 GPa, and 13.6 GPa, respectively, which are 30 %, 12.4 %, and 7.4 % higher than that of R-0GP specimens, respectively. However, the addition of GP has no obvious effect on the elastic modulus of the old mortar.

4 Discussion

The mechanism for increasing the mechanical properties of RAC using GP includes the following physicochemical aspects: (1) Filling effect. GP has a smaller particle size than cement particles (Fig. 1); this facilitates the filling of pores between unhydrated cement particles. (2) Pozzolanic effect. GP contains a large amount of amorphous SiO_2 (Table 1). In an alkaline solution, Si^{4+} ions precipitated from GP are efficiently rehydrated with the hydration product CH to form additional C–S–H gels to fill pores; thus, the compactness of the RAC matrix is improved (Fig. 6). As described above for MIP, specimens containing GP have a lower porosity (Fig. 7 and Table 3); (3) Improving the ITZ. The results of nanoindentation show that incorporation of GP enhances the bond between old and new mortar, reduces the width of the ITZ, and increases the average elastic modulus of the ITZ (Fig. 8).

In this work, the drying shrinkage and creep of RAC specimens were measured for 180 days to evaluate the volume stability of RAC. For the RAC in the unconstrained state, the drying shrinkage ε_d is as follows:

$$\varepsilon_d = \frac{\sigma_i}{E_c}, \quad (3)$$

where σ_i is the internal stress, and E_c is the elastic modulus. The internal stress of porous materials is caused by capillary pressure:

$$\sigma_i = -\frac{V}{1-V}p_{surf}, \quad (4)$$

where V is the relative volume of pores smaller than 50 nm; previous studies have reported that pores smaller than 50 nm play an essential role in drying shrinkage [29]. p_{surf} is the surface pressure given by the Kelvin-Laplace equation [33].

$$p_{surf} = \frac{2\alpha\cos\theta}{r}, \quad (5)$$

Here α is the surface tension of the pore solution, θ is the contact angle between liquid and solid, and r is the radius of a capillary pore. Substituting Eqs (4) and (5) into Eq (3), we can obtain:

$$\varepsilon_d = -\frac{V}{1-V}\cdot\frac{2\alpha\cos\theta}{E_c}. \quad (6)$$

The degree of drying shrinkage should be

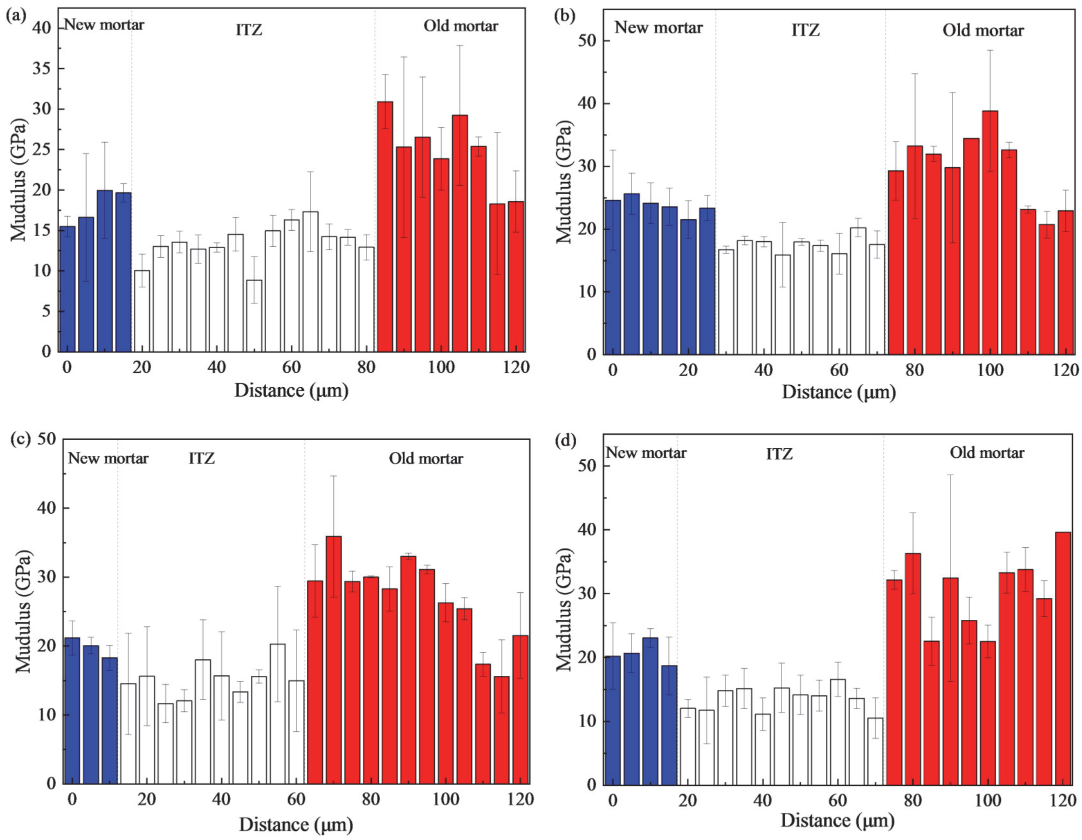

Fig.8. Widths of ITZ for RAC: (a) R-0GPa 65m, (b) R-10GPa, 55m, (c) R-20GPa, 45m, and (d)R-30GPa, 50m.

$$\varepsilon_d = \frac{V}{1-V} \cdot \frac{2\alpha\cos\theta}{E_c}. \quad (7)$$

According to the above formula, the drying shrinkage of concrete is inversely proportional to the fine pore volume and the elastic modulus. Table 4 summarizes dry shrinkage, creep, volume of fine pores, and elastic modulus of RAC. With the addition of GP, the dry shrinkage and creep properties of RAC are significantly improved. With the addition of the proper amount of GP, RAC can achieve a higher elastic modulus, lower small pore volume (< 50 nm), which is improves the shrinkage resistance of the RAC matrix, thereby reducing the dry shrinkage and creep characteristics of the RAC. However, excess GP replacing cement reduces the amount of cement used, resulting in fewer hydration products, and weakening the microstructure of RAC. It can be found that compared with the 10 % GP specimen, the 30 % GP specimen has a higher volume of fine pores (< 50 nm) and elastic modulus, resulting in the increased dry shrinkage and creep.

Conclusion

This paper studied the effects of GP on the mechanical properties, drying shrinkage and creep of RAC. The microstructure of

Table 4. Drying shrinkage, creep, pore volume (<50 nm), and elastic modulus

Sample	Drying shrinkage, μ_ε	Creep, μ_ε	Pore volume (<50 nm), mL/g	Elastic modulus, GPa
R-0GP	312.6	746.1	0.0836	32.65
R-10GP	242.0	533.4	0.0427	33.32
R-20GP	258.6	560.8	0.0498	32.91
R-30GP	277.7	638.8	0.0453	31.85

RAC was determined by MIP and nanoindentation techniques. The results show that:

(1) The addition of GP reduced the compressive strength of RAC at the early stage, but increased the compressive strength at the later stage. The specimens containing 10 % GP showed the best compressive strength. With the further increase of the GP content, the compressive strength of RAC decreased gradually, and for the specimens containing 30 % GP, the results were lower than the control group. The variation trend of the splitting strength and elastic modulus of RAC is similar to that of the compressive strength. The polygonal shape of the GP increases the setting force and the bonding effect between the aggregate and the matrix and increases the brittleness of the RAC.

(2) The drying shrinkage of RAC can be lowered by adding the appropriate amount of GP. Compared with the R-0GP, the drying shrinkage of specimens containing 10 %, 20 %, and 30 % GP decreased by 19.7 %, 17.3 %, and 11.4 %, respectively, after 180 days. The creep of RAC was reduced by adding the appropriate GP amount. Compared with the R-0GP, the 180 day creep strain and the creep coefficient of the GP specimens are reduced by 11.4 ~ 26 % and 2.2 % ~ 24.4 %, respectively. However, excessive GP increases the creep degree of RAC.

(3) MIP analysis showed that adding GP improved the RAC microstructure, and the porosity (larger than 100 nm) of specimens containing 10 % and 20 % GP decreased compared with the control group. However, samples containing 30 % GP increased porosity at a pore size of more than 100 nm. The nanoindentation test results show that the width of the ITZ in RAC decreases by 15.4 %, 30.85 and 23.1 % with GP incorporation, respectively, due to the pozzolanic effect and filling effect of GP.

Author Contributions: Conceptualization, Investigation (Qidong Wang); Data curation, Writing-original draft, and Funding acquisition (Minghua Yang); Visualization, Writing-review, and editing (Xudong Wang). All authors have read and agreed to the published version of the manuscript.

Funding: This work was financially supported by the National Natural Science Foundation of Zhejiang province (Grant No. LHY22E080001)

Acknowledgments: The authors are grateful for the financial support from the National Natural Science Foundation of Zhejiang province.

Conflicts of Interest: The authors declare that they have no competing financial interest conflicts in this paper.

References

1. P.Zhan, J.Xu, J.Wang et al., *J.Clean Prod.*, **375**, 134116 (2022).
2. I.B.Topcu, S.Sengel, *Cem.Concr.Res.*, **34**, 1307 (2004).
3. W.He, G.Liao, *Funct.Mater.*, **28**, 737 (2021).
4. J.Xiao, H.Li, Z.Yang, *Construction and Building Materials*, **38**, 681 (2013).
5. X.F.Yuan, G.Liao, *Funct.Mater.*, **29**, 268 (2022).
6. J.de Brito, R.Robles, *Indian Journal of Engineering and Materials Sciences*, **17**, 449 (2010).
7. V.I.Sokolenko, E.V.Karaseva, A.V.Mats et al., *Funct.Mater.*, **24**, 256 (2017).
8. L.Evangelista, J.de Brito, *Cem.Concr.Compos.*, **32**, 9 (2010).
9. O.Cakir, *Construction and Building Materials*, **68**, 17 (2014).
10. R.V.Silva, J.de Brito, R.K.Dhir, *Journal of Cleaner Production*, **112**, 2171 (2016).
11. M.Shariq, J.Prasad, H.Abbas, *Cem.Concr. Compos.*, **68**, 35 (2016).
12. Z.-h.He; L.-y.Li; S.-g.Du, *Cem.Concr.Compos.*, **80**, 190 (2017).
13. A.M.Rashad, *Construction and Building Materials*, **72**, 340 (2014).
14. S.B.Park, B.C.Lee, J.H.Kim, *Cem.Concr.Research*, **34**, 2181 (2004).
15. M.Mirzahosseini, K.A.Riding, *Cement & Concrete Composites*, **56**, 95 (2015).
16. M.Carsana, M.Frassoni, L.Bertolini, *Cem. Concr.Compos.*, **45**, 39 (2014).
17. M.Mirzahosseini, K.A.Riding, *Cem.Concr. Res.*, **58**, 103 (2014).
18. A.F.Omran, E.D.Morin, D.Harbec, A.Tagnit-Hamou, *Construction and Building Materials*, **135**, 43 (2017).
19. M.Kamali, A.Ghahremaninezhad, *Construction and Building Materials*, **98**, 407 (2015).
20. N.Schwarz, H.Cam, N.Neithalath, *Cem.Concr. Compos.*, **30**, 486 (2008).
21. A.Omran, D.Harbec, A.Tagnit-Hamou, R.Gagne, *Construction and Building Materials*, **133**, 450 (2017).
22. H.-Y.Wang, H.-H.Zeng; J.-Y.Wu, *Construction and Building Materials*, **50**, 664 (2014).
23. A.A.Aliabdo, A.E.M.Abd Elmoaty, A.Y.Aboshama, *Construction and Building Materials*, **124**, 866 (2016).
25. J.-X.Lu, B.-J.Zhan, Z.-H.Duan, C.S.Poon, *Materials & Design*, **135**, 102 (2017).
25. G.S.Islam, M.Rahman, N.Kazi, *International Journal of Sustainable Built Environment*, **6**, 37 (2017)

26. W.Qidong, Z.Changshun, W.Xudong et al., *Materials Research Express*, **9**, 075008 (2022).
27. J.Xu, B.Wang, J.Zuo, *Cem.Concr.Compos.*, **81**, 1 (2017).
28. G.Liang, T.Liu, H.Li, K.Wu, *Composites Part B: Engineering*, **231**, 109570 (2022).
29. Z.He, P.Zhan, S.Du et al., *Composites Part B-Engineering*, **166**, 13 (2019)
30. P.Zhan, J.Xu, J.Wang, C.Jiang, *Construction and Building Materials*, **307**, 125082 (2021).
31. P.Mondal, S.P.Shah, L.Marks, *Cem.Concr. Res.*, **37**, 1440 (2007).
32. W.Tang, J.Shi, Z.He et al., *AcMCS*, **39**, 2369 (2022).
33. C.Hua, P.Acker, A.Ehrlacher, *Cement Concrete Research*, **25**, 1457 (1995).